



## Simulation, Fabrication and Mechanical Characterization of a Jute–Epoxy Biocomposite Hubcap for Automotive Applications

Nafissa Moussaoui , Salah Amroune, Ahmed Belaadi , Moussa Zaoui ,  
Mohammad Jawaid , Mahmood M. S. Abdullah , Hamad A. Al-Lohedan ,  
Herbert Mukalazi & Amar Al-Khawlani

**To cite this article:** Nafissa Moussaoui , Salah Amroune, Ahmed Belaadi , Moussa Zaoui ,  
Mohammad Jawaid , Mahmood M. S. Abdullah , Hamad A. Al-Lohedan , Herbert Mukalazi &  
Amar Al-Khawlani (2026) Simulation, Fabrication and Mechanical Characterization of a Jute–  
Epoxy Biocomposite Hubcap for Automotive Applications, Journal of Natural Fibers, 23:1,  
2672672, DOI: [10.1080/15440478.2026.2672672](https://doi.org/10.1080/15440478.2026.2672672)

**To link to this article:** <https://doi.org/10.1080/15440478.2026.2672672>



© 2026 The Author(s). Published with  
license by Taylor & Francis Group, LLC.



Published online: 14 May 2026.



Submit your article to this journal [↗](#)



Article views: 14



View related articles [↗](#)



View Crossmark data [↗](#)

## Simulation, Fabrication and Mechanical Characterization of a Jute–Epoxy Biocomposite Hubcap for Automotive Applications

Nafissa Moussaoui<sup>a</sup>, Salah Amroune<sup>a,b</sup>, Ahmed Belaadi<sup>c</sup>, Moussa Zaoui<sup>a</sup>, Mohammad Jawaid<sup>d</sup>, Mahmood M. S. Abdullah<sup>e</sup>, Hamad A. Al-Lohedan<sup>e</sup>, Herbert Mukalazi<sup>f</sup>, and Amar Al-Khawlani<sup>g</sup>

<sup>a</sup>Mechanical Department, Faculty of Technology, University of Msila, Algeria; <sup>b</sup>Materials and Structural Mechanics Laboratory (LMMS), University of Msila, Algeria; <sup>c</sup>Department of Mechanical Engineering, Faculty of Technology, University 20 Aout 1955-Skikda, El-Hadaiek Skikda, Algeria; <sup>d</sup>Chemical and Petroleum Engineering Department, College of Engineering, United Arab Emirates University (UAEU), Al Ain, United Arab Emirates; <sup>e</sup>Department of Chemistry, College of Science, King Saud University, Riyadh, Saudi Arabia; <sup>f</sup>Department of Mathematics and Statistics, Kyambogo University, Kampala, Uganda; <sup>g</sup>Jiangsu Optoelectronic Functional Materials and Engineering Research Centre, School of Chemistry and Chemical Engineering, Southeast University, Nanjing, China

### ABSTRACT

This study presents the design, numerical simulation, fabrication, and mechanical characterization of an automotive hubcap manufactured from a jute fabric-reinforced epoxy biocomposite. The hubcap geometry was designed in SolidWorks and analyzed using finite element simulations under static, centrifugal (2546 rpm), and thermal (130 °C) loading conditions representative of service environments. The component was fabricated by compression molding using a two-part silicone mold derived from a 3D-printed master. Mechanical testing of jute–epoxy laminates revealed a tensile strength of 25.97 MPa, a tensile modulus of 2.47 GPa, a flexural strength of 69.41 MPa, and a flexural modulus of 1.08 GPa. Finite element results showed low deformation (maximum 0.058 mm under static load and 0.031 mm under centrifugal load) and Von Mises stresses below 9.5 MPa, corresponding to safety factors above 2.7. Under thermal loading, the maximum stress reached 52.3 MPa with a displacement of 0.138 mm, identifying temperature as the most critical condition. The fabricated hubcap exhibited a low mass of 239 g, representing an estimated weight reduction of 30–40% compared to conventional plastic alternatives. These results confirm the feasibility of jute-based biocomposites for lightweight, non-structural automotive applications with improved environmental performance.

### 摘要

本研究針對一種由黃麻織物增強環氧生物複合材料製成的汽車輪轂蓋，闡述其設計、數值模擬、製造及力學特性分析。輪轂蓋的幾何形狀在SolidWorks中進行設計，並透過有限元素模擬，在代表實際使用環境的靜態、離心 (2546rpm)及熱 (130 °C) 載荷條件下進行分析。該部件採用由3D列印母模衍生的雙組分矽膠模具，透過壓縮成型製成。對黃麻-環氧樹脂層壓板的機械測試顯示，其抗拉強度為25.97 MPa、抗拉模量為2.47 GPa、彎曲強度為69.41 MPa，以及彎曲模量為1.08 GPa。有限元素分析結果顯示，其變形量較小 (靜態載荷下最大0.058 mm，離心載荷下最大0.031 mm)，馮·米塞斯應力低於9.5 MPa，對應的安全係數高於2.7。在熱載荷作用下，最大應力達52.3 MPa，位移為0.138 mm，表明溫度是關鍵的工況。所製成的輪轂蓋重量僅 239 克，相較於傳統塑膠替代品，估計減重幅度達 30–40%。這些結果證實了以黃麻為基材的生物複合材料，適用於輕量化、非結構性的汽車應用，並能提升環境性能。

### KEYWORDS

Jute fabric-reinforced epoxy; automotive hubcap; natural fiber biocomposite; thermo-mechanical finite element analysis; compression molding process; tensile and flexural characterization; lightweight automotive components

### 關鍵詞

黃麻布增強環氧樹脂; 汽車輪轂蓋; 天然纖維生物複合材料; 熱力學與力學有限元素分析; 壓縮成型工藝; 拉伸與彎曲特性分析; 輕量化汽車零組件

## Introduction

The automotive industry faces increasing pressure to reduce vehicle mass, fuel consumption and greenhouse-gas emissions while maintaining high standards of safety, comfort, and durability. Fiber-reinforced polymer (FRP) composites based on glass or carbon fibers are widely used because of their high specific stiffness and strength, yet their nonrenewable origin, energy-intensive production and difficult end-of-life management raise environmental concerns (Czerwinski 2021;

**CONTACT** Ahmed Belaadi ✉ [ahmedbelaadi1@gmail.com](mailto:ahmedbelaadi1@gmail.com) Department of Mechanical Engineering, Faculty of Technology, University 20 Aout 1955-Skikda, El-Hadaiek Skikda 21000, Algeria; Herbert Mukalazi ✉ [hmukalazi@kyu.ac.ug](mailto:hmukalazi@kyu.ac.ug) Department of Mathematics and Statistics, Kyambogo University, Kampala, Uganda

© 2026 The Author(s). Published with license by Taylor & Francis Group, LLC.

This is an Open Access article distributed under the terms of the Creative Commons Attribution License (<http://creativecommons.org/licenses/by/4.0/>), which permits unrestricted use, distribution, and reproduction in any medium, provided the original work is properly cited. The terms on which this article has been published allow the posting of the Accepted Manuscript in a repository by the author(s) or with their consent.

Mostefa Meddah et al. 2026; Musa and Onwualu 2024; Skosana, Khoathane, and Malwela 2025; Yan and Xu 2025). Natural-fiber-reinforced biocomposites have therefore emerged as promising alternatives, combining low density, partial biodegradability, and a reduced carbon footprint (Akter, Uddin, and Tania 2022; Naghdi 2021; Puttegowda 2025; Saravanakumar et al. 2026). Lignocellulosic fibers such as jute, flax, hemp, Inula and sisal have been extensively investigated as reinforcements for thermoplastic and thermoset matrices (Amroune et al. 2021; Belaadi et al. 2022; Benyettou et al. 2026; Fnides et al. 2026; Kurien, Selvaraj, et al. 2023; Lamia et al. 2023; Moussaoui et al. 2021). Their relatively low density (about 1.3–1.5 g/cm<sup>3</sup> for jute) and tensile strength typically between 350 and 800 MPa offer attractive stiffness-to-weight ratios for semi-structural components. Recent reviews underline that natural-fiber biocomposites can achieve mechanical performance compatible with many automotive applications, while reducing part weight by 20–40% compared with glass-fiber composites (Islam et al. 2022; Kurien and Thomas 2026; Kurien et al. 2022, Ullah, Akhter et al. 2025; Kurien et al. 2026). However, the overall behavior of these materials is often limited by moisture sensitivity, variability of fiber properties and imperfect fiber–matrix adhesion, which can lead to premature damage under severe mechanical or thermal loading as clearly shown by the evolution of interfacial strength and crack-propagation resistance after physico-chemical and alkali treatments on new cellulosic fibers (Azwa et al. 2013; Benhamadouche et al. 2025; Madueke, Mbah, and Umunakwe 2023; Sivaraja et al. 2010).

Among natural fibers, jute is particularly attractive thanks to its widespread availability, low cost, good specific mechanical properties, and compatibility with common polymer matrices. Several studies have reported that jute–epoxy laminates can reach tensile strengths in the 25–80 MPa range and flexural strengths above 70 MPa, depending on fiber content, fabric architecture and processing conditions (Belaadi et al. 2020; Gupta et al. 2023; Kannan, Thangaraju, et al. 2025; Kurien, Arshad, et al. 2025; Slamani et al. 2025). Such properties make jute–epoxy biocomposites suitable for semi-structural components where weight, stiffness and impact resistance must be balanced with sustainability requirements. At the same time, the relatively low glass transition temperature and thermal stability of standard epoxy systems raise questions about their behavior in exterior automotive environments, where components are exposed to temperature gradients, solar radiation, and thermal cycling. Similar tensile and flexural levels have been reported for newly developed cellulosic fibers extracted from date-palm spathes and other agricultural by-products, once appropriate extraction, and alkali or physico-chemical treatments are applied, confirming that well-engineered lignocellulosic reinforcements can compete with traditional bast fibers in biocomposites (Djalal et al. 2024; Moussaoui et al. 2023; Musa and Onwualu 2024; Naik and Kumar 2021; Raja et al. 2025).

Natural-fiber biocomposites are already used in interior automotive parts such as door panels (Kurien et al. 2020), instrument-panel carriers and trunk liners, and they are increasingly considered for exterior components including bumpers, underbody shields and body panels. Nevertheless, their potential for smaller exterior accessories such as hubcaps (wheel covers) remains less explored, even though these parts are relevant for light-weighting and aesthetic customization and are subjected to combined mechanical, centrifugal, and thermal loads during service (Kannan, Kurien, et al. 2025; Kurien, Bodaghi, et al. 2025; Kurien, Maria Anil, et al. 2023). In particular, there is a lack of studies that combine detailed mechanical characterization of jute–epoxy composites, finite element analysis of realistic hubcap geometries and experimental fabrication of full-scale prototypes (Fisher 2023; Kurien et al. 2024; Musa and Onwualu 2024, Sahu, Das et al. 2025; Naik and Kumar 2021; Skosana, Khoathane, and Malwela 2025).

This work addresses a gap by presenting an original study of a full-scale automotive hubcap made entirely from a jute–epoxy biocomposite. Its originality lies in an integrated approach combining design, experimental characterization, numerical modeling, and validation through a functional prototype. The main contributions are: (i) the design of a geometry adapted to the mechanical and thermal constraints of exterior applications; (ii) the determination of tensile and flexural properties of the laminate, implemented in an equivalent finite element model; (iii) a detailed numerical analysis under combined static, centrifugal, and thermal loading; and (iv) the fabrication of a prototype by compression moulding using a silicone mold derived from 3D printing. This approach provides a realistic basis for replacing conventional plastic hubcaps.

## Methodology

### Materials

#### Jute fabric

Jute is a lignocellulosic fiber obtained from plants of the genus *Corchorus*. It is widely used in polymer composites due to its favorable balance between mechanical properties, cost, and renewability. The woven jute fabric employed in this study exhibits a density of about  $1.3\text{--}1.5\text{ g/cm}^3$ , a tensile strength between 393 and 800 MPa, and a Young's modulus ranging from 10 to 30 GPa, as reported in earlier characterization studies. The fabric architecture provides multidirectional reinforcement and promotes uniform impregnation by the epoxy matrix (Figure 1a).

#### Epoxy matrix (MEDAPOXY STR)

The MEDAPOXY STR epoxy system, supplied by GRANITEX–GNP (Algiers, Algeria), is used as thermoset matrix. It is provided as a pre-dosed two-component kit consisting of resin (component A) and hardener (component B), offering good chemical resistance, strong adhesion to various substrates and excellent wettability of fibrous reinforcements (Figure 1a, b). The resin/hardener mass ratio recommended by the manufacturer (100:40) is adopted throughout the study.

#### Hubcap design

The hubcap is designed in SolidWorks following a systematic procedure based on functional analysis and service constraints. The main functions are: (i) protection of the wheel hub and nuts against debris and corrosion, (ii) enhancement of wheel aesthetics, and (iii) contribution to vehicle lightweighting through an optimized geometry. Design constraints include resistance to dynamic loading, compatibility with a five-stud rim, thermal resistance up to  $100^\circ\text{C}$  and ease of assembly/removal during maintenance.

A technical specification is derived from these requirements, setting a nominal diameter of 380 mm, an average thickness of 2–3 mm and a target mass below 500 g. The 3D model is generated from a 2D sketch revolved around the wheel axis, followed by 3D operations including fillets to reduce stress concentrations, peripheral cutouts to decrease weight and maintain stiffness, and bolt-hole patterns matching the rim geometry. Figure 2 shows the final CAD model with five uniformly distributed fixing points around the hub and peripheral openings for weight reduction and visual effect.

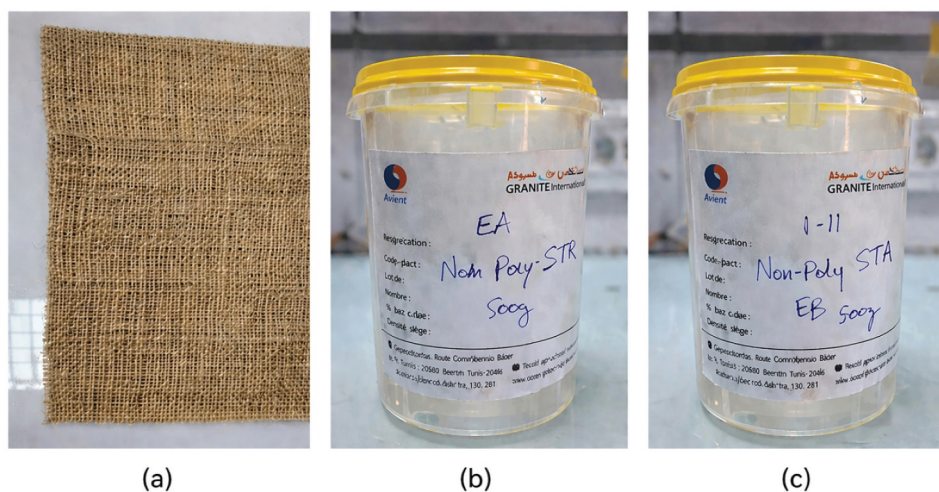


**Figure 1.** (a) jute fabric used as reinforcement for the biocomposite hubcap, MEDAPOXY str epoxy system: component a (resin) and component B (hardener).

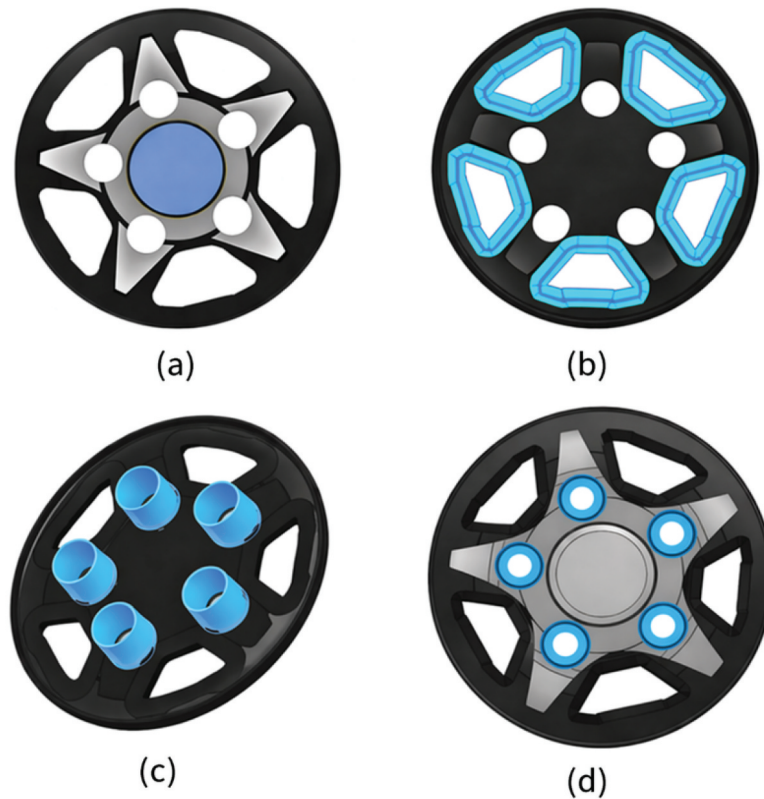


**Figure 2.** CAD model of the biocomposite hubcap designed in SolidWorks: (a) base hubcap structure, (b) fiber-reinforced regions, (c) insertion of cylindrical reinforcement elements, and (d) final assembled hubcap design.

### **Finite element simulation**

A finite element (FE) analysis is conducted using SolidWorks Simulation to evaluate the structural response of the jute–epoxy hubcap under representative service conditions. The material is modeled as an equivalent homogeneous medium, whose properties are derived from the experimentally measured tensile and flexural characteristics of the composite (Governing equations) and supplemented with data reported in the literature for comparable natural fiber laminates (Farronato et al. 2019; Ibrahim et al. 2025; Saada et al. 2023; Sahu and Mohanty 2025; Siguerdjidjene et al. 2024).). Boundary conditions are imposed at the five attachment regions, which are idealized as fixed supports to simulate the rigid clamping of the hubcap onto the wheel rim (Sahu, Das et al. 2025; Sahu, Das, and Mohanty 2025).

Three loading scenarios are investigated: (i) a static mechanical load representing in-service forces, (ii) a centrifugal load associated with a rotational speed of 2546 rpm, and (iii) a uniform thermal load of 130°C to account for heating effects induced by braking and environmental conditions. The hubcap geometry is discretised using three-dimensional tetrahedral finite elements, a choice driven by the geometric complexity of the component, including curved surfaces, fillets, and local discontinuities near the fixing holes. These elements are well suited to irregular geometries, allowing efficient automatic mesh generation and good adaptability, while enabling local refinement in critical to accurately capture stress concentrations. This strategy provides a suitable compromise between computational cost and solution accuracy within the SolidWorks Simulation framework (Figure 3) (Belhocine and Abdullah 2020; Koppiseti, Nallu, and Penmetsa 2022; Shinde, Bulsara, and Patil 2022). For each loading case, the FE solver yields the distributions of Von Mises stresses, displacement fields, and corresponding safety factors relative to the admissible strength of the composite.

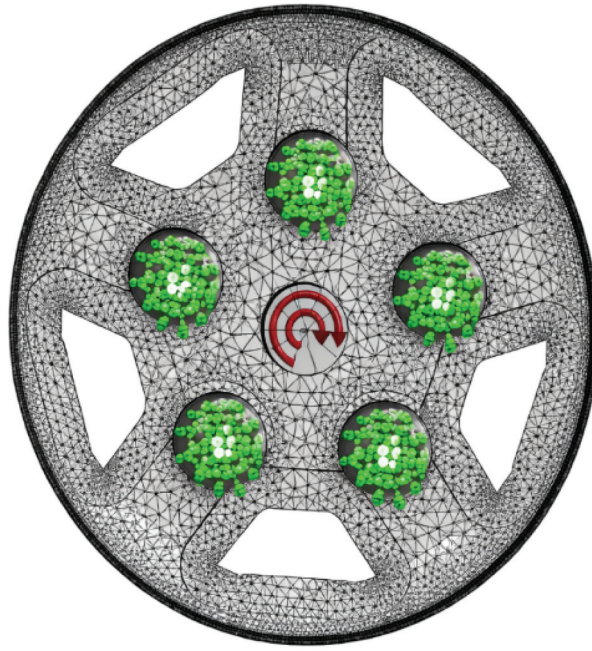


**Figure 3.** Finite element mesh of the hubcap with local refinement near fixing holes and geometric details.

### **Mathematical formulation and finite element modeling**

The mathematical behavior of the hubcap structure is analyzed using the finite element method under the framework of linear thermoelasticity. The material is assumed to be homogeneous and linearly elastic, and small deformations are considered (Awrejcewicz and Krysko 2020; Dunić et al. 2016; Sánchez-Majano et al. 2022).

### **Governing equations**

Let  $\Omega \subset \mathbb{R}^3$  denote the domain of the structure with bounding  $\partial\Omega = \Gamma_u \cup \Gamma_t$  where  $\Gamma_u$  represents the fixed regions corresponding to the five attachment points. The unknown field is the displacement vector  $U(x)$

The strain tensor is defined as (eq. 1):

$$\varepsilon(U) = \frac{1}{2} (\Delta U + (\Delta U)^T) \quad (1)$$

The constitutive relation for linear thermoelasticity is given by (eq. 2):

$$\sigma = C : (\varepsilon(u) - \varepsilon^{th}) \quad (2)$$

Where  $C$  is the fourth-order elasticity tensor and  $\varepsilon^{th}$  is the thermal strain tensor. For an isotropic material, the thermal strain reads (eq.3):

$$\varepsilon^{th} = \alpha \Delta T I \quad (3)$$

With  $\alpha$  being the coefficient of thermal expansion,  $\Delta T = T - T_{ref}$ , and  $I$  the second-order identity tensor. The equilibrium equation in the absence of inertia effects is expressed as:

$$\Delta \cdot \sigma + b = 0 \text{ in } \Omega$$

Where  $b$  denotes the body force vector.

The bonding conditions are defined as:

$$u = 0 \text{ on } \Gamma_u$$

$$\sigma n = t \text{ on } \Gamma_t$$

Where  $n$  is the outward normal to the boundary and  $t$  is the applied traction vector.

### Load cases

Three loading configurations are considered:

- (1) **Static mechanical loading**, applied as external forces or pressures on selected surfaces.
- (2) **Centrifugal loading**, associated with rotational motion at an angular velocity  $\omega$ . The centrifugal body force is expressed as (Eq. 4):

$$b(x) = \rho\omega^2 r(x)e_r \quad (4)$$

Where  $\rho$  is the material density,  $r(x)$  is the radial distance from the axis of rotation, and  $e_r$  is the radial unit vector.

**Thermal loading**, corresponding to a uniform temperature increase applied to the structure, generating thermal strain due to constrained deformation.

### Weak form and finite elements discretization

The weak form of equilibrium problem is obtained using the principal of virtual work. Find  $u \in [H^1(\Omega)]^3$  such that  $u = 0$  on  $\Gamma_u$  and for all admissible virtual displacement  $v \in [H^1(\Omega)]^3$  vanishing on  $\Gamma_u$  the following holds (Eq.5):

$$\int_{\Omega} \varepsilon(v) : C : \varepsilon(u) d\Omega = \int_{\Omega} v \cdot b d\Omega + \int_{\Gamma_t} v \cdot t d\Gamma + \int_{\Omega} \varepsilon(v) : C : \varepsilon^{th} d\Omega \quad (5)$$

The domain is discretized using three-dimensional finite elements, leading to the following system of algebraic equations.

$$KU = F_{mec} + F_{cent} + F_{th}$$

Where  $K$  is the global stiffness matrix,  $U$  is the nodal displacement vector, and  $F_{mec}$ ,  $F_{cent}$ , and  $F_{th}$  are the mechanical, centrifugal, and thermal load vectors, respectively.

### Post processing

The stress condition within the material is assessed by calculating the von Mises equivalent stress, which serves as a scalar indicator derived from the different normal and shear stress components and is mathematically expressed as follows (Eq.6):

$$\sigma_{VM} = \sqrt{\frac{1}{2}[(\sigma_{xx} - \sigma_{yy})^2 + (\sigma_{yy} - \sigma_{zz})^2 + (\sigma_{zz} - \sigma_{xx})^2 + 3(\tau_{xy}^2 + \tau_{yz}^2 + \tau_{zx}^2)]} \quad (6)$$

### Manufacturing of the hubcap

#### Master and silicone mold – 3D printed

A master model of the hubcap is produced by fused-deposition modeling (FDM) using the CAD geometry exported to slicing software. The printed part serves as a physical template for subsequent silicone molding (Figure 4).

A two-part silicone mold is then manufactured in two phases: in the first phase, the printed master is fixed to a rigid base plate, placed in a sealed box and partially embedded in silicone to form the first half of the mold; in the second phase, a release agent is applied, the master is repositioned using alignment dowels, and the second half of the silicone is poured and cured, resulting in a reusable mold with accurate geometry (Figure 5).

#### Compression molding of the jute–epoxy hubcap

The hubcap is manufactured by compression molding using the silicone mold and two jute fabric plies cut to the final geometry. The plies (~1.5 mm thick) are punched according to the hubcap pattern (diameter 380 mm, five fixing holes  $\varnothing$  12 mm) and dried under controlled pressure (2 MPa, 80°C, 10 min) in a hydraulic press to remove residual moisture and stabilize the fibers. The epoxy resin and hardener

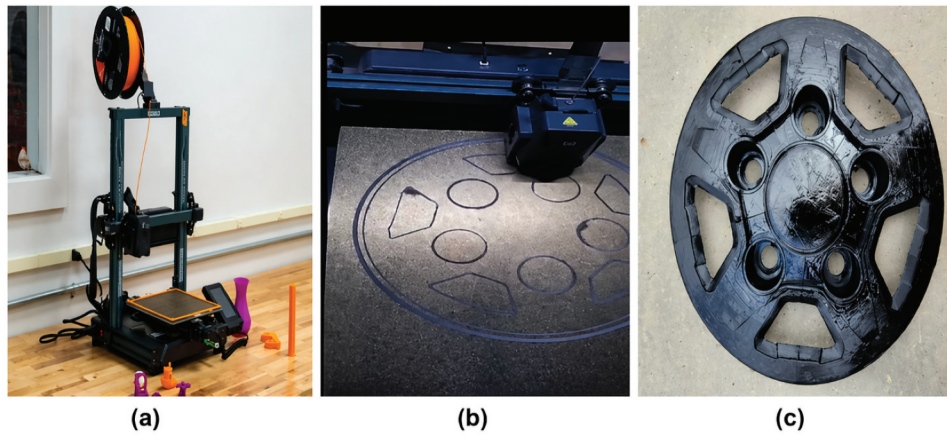


**Figure 4.** 3D printed master model of the hubcap used to fabricate the silicone mold: (a) 3D printer setup, (b) printing process of the hubcap model, and (c) final 3D printed hubcap master model.

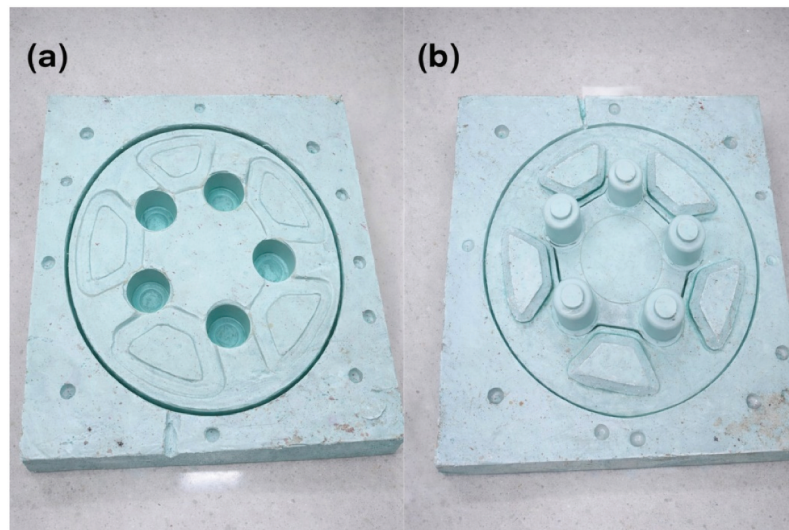


**Figure 5.** Two-part silicone mould of the hubcap: (a) first half; (b) second half.

(100:40 mass ratio) are mixed thoroughly and degassed under vacuum to minimize air entrapment. The dried jute plies are impregnated manually on both sides with the epoxy system to ensure full saturation, and the [jute/resin/jute] lay-up is placed inside the silicone mold.

The mold is closed and subjected to isothermal compression (3 MPa, 60°C, 4 h), followed by cooling at room temperature for 12 h. After demolding, the hubcap is trimmed, sanded (P400) and cleaned to reach an automotive-grade surface finish ( $R_a < 3.2 \mu\text{m}$ ) (Figure 6). The final mass of the hubcap is measured as 239 g.

### **Mechanical testing of jute–epoxy plates**

Rectangular tensile and flexural specimens were machined from jute–epoxy plates manufactured under the same processing and curing conditions as the hubcap. The tensile tests were performed in accordance with ASTM D3039, using specimens with a gauge length of 100 mm, a width of 15 mm and a nominal thickness of 3 mm, while three-point bending tests followed ASTM D790 with a span-to-thickness ratio of 16:1 (Faruk et al. 2012; Pickering, Efendy, and Le 2016; Saba et al. 2016). All tests were conducted on a universal testing machine equipped with a 5 kN load cell at a constant crosshead speed of 2 mm/min. For each configuration, at least four specimens were tested to account for variability, and average values as well as standard deviations of Young's modulus and ultimate strength were calculated (Figure 7). The measured tensile



**Figure 6.** Compression moulding and final biocomposite hubcap after demoulding and finishing.

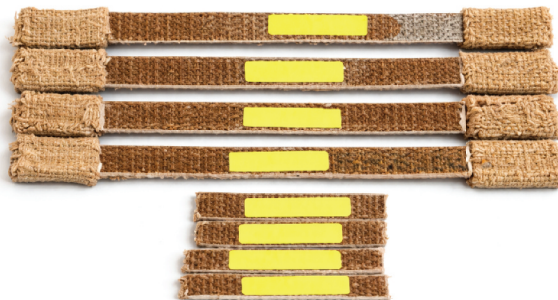


**Figure 7.** Test specimens for tensile and flexural testing.

and flexural properties were then used as input data for defining the equivalent homogeneous material in the finite element simulations

## Results and discussion

### *Mechanical properties of the jute–epoxy composite*

The mechanical characterization of the jute–epoxy laminate shows a tensile Young’s modulus of approximately 2.47 GPa and an ultimate tensile strength of 25.97 MPa, while the flexural modulus and flexural strength reach 1.08 GPa and 69.41 MPa, respectively. These values fall within the typical range reported for woven jute–epoxy laminates (Benhamadouche et al. 2025; Joshi et al. 2004; Karthika, Deb, and Venkatesh 2021; Mir et al. 2010), confirming both the consistency of the material and the reliability of the manufacturing process adopted in this study. From a materials engineering perspective, the combination of moderate strength and satisfactory stiffness reflects the intrinsic characteristics of natural-fiber composites, which generally exhibit lower absolute mechanical performance than synthetic fiber composites but offer competitive specific properties. This balance makes the material particularly suitable for semi-structural

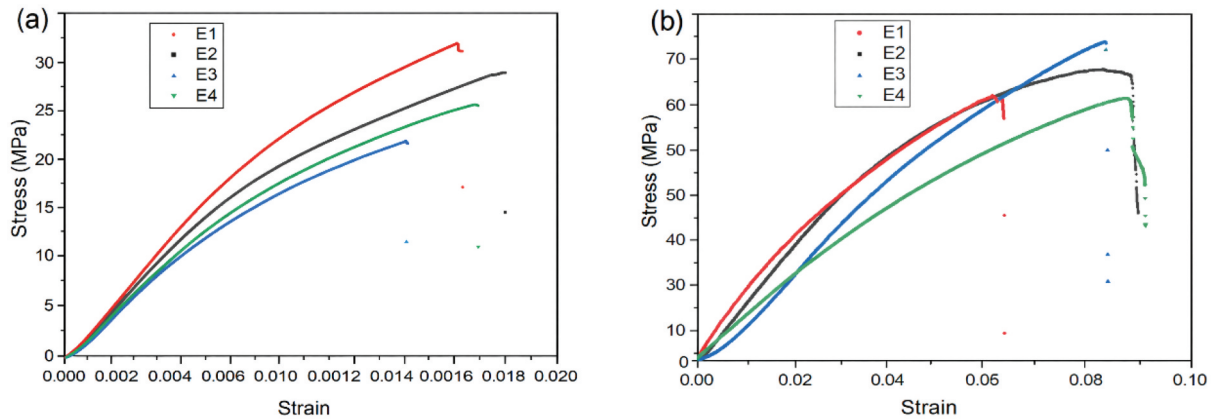


**Figure 8.** (a) tensile stress–strain curves of specimens E1–E4, (b) flexural stress–strain curves of specimens E1–E4.

applications where weight reduction and sustainability are key considerations. The tensile stress–strain curves of specimens E1–E4 (Figure 8a) exhibit an initial quasi-linear elastic region up to approximately 15–20 MPa, corresponding to the elastic response of both the epoxy matrix and the jute fibers with effective stress transfer at the fiber–matrix interface. Beyond this stage, a gradual deviation from linearity is observed, indicating the onset of damage mechanisms such as matrix micro-cracking, fiber–matrix debonding and local fiber reorientation within the woven structure. The final stage is characterized by a pseudo-ductile failure occurring between approximately 22 and 32 MPa at strains ranging from 0.012 to 0.017. This progressive failure behavior is typical of woven natural-fiber composites and has been widely reported in the literature (Haq et al. 2024; Hasan, Islam, and Hassan 2024), and is advantageous in terms of structural safety as it prevents sudden brittle fracture.

The variability observed between the different tensile curves can be attributed to the inherent heterogeneity of natural fibers as well as to processing-related factors. Differences in fiber properties, such as diameter, microfibril angle and cellulose content, combined with potential variations in impregnation quality, void content and fiber alignment, contribute to the dispersion of the results. Such variability is a well-known characteristic of lignocellulosic composites and must be accounted for in engineering design through appropriate safety factors (Haq et al. 2024; Hasan, Islam, and Hassan 2024). In practice, the allowable stress is often limited to a fraction (around 30–40%) of the ultimate tensile strength to ensure structural reliability under service conditions.

The flexural behavior of the laminate, illustrated in Figure 8b, is particularly relevant for the hubcap application, which is mainly subjected to bending loads. The flexural stress–strain curves display an initially linear response followed by a non-linear regime and pseudo-ductile failure, similar to the tensile behavior but with higher stress levels, reaching up to about 69.41 MPa. This higher resistance in bending can be explained by the laminated structure, where the outer plies sustain tensile and compressive stresses while the inner layers contribute to shear transfer. Failure mechanisms under bending involve tensile cracking of the outer layers, fiber micro-buckling in compression and interlaminar debonding, as commonly reported for woven natural-fiber laminates (Abdellaoui et al. 2015; Hossain et al. 2013).

Overall, the mechanical performance of the jute–epoxy laminate demonstrates a suitable compromise between stiffness, strength, weight and environmental benefits. These results confirm the potential of such biocomposites for non-structural automotive components such as hubcaps, where moderate mechanical performance combined with lightweight characteristics and sustainability is required, in agreement with recent developments in natural-fiber composites for automotive applications (Ullah, Akhter et al. 2025).

### **Structural performance of the jute–epoxy hubcap**

The FE analysis allows the structural response of the hubcap to be evaluated under three representative loading scenarios: static mechanical load, centrifugal load at 2546 rpm and uniform thermal load at 130°C. Under static loading, Von Mises stresses range from 600 Pa to 8 MPa, with the highest values localized

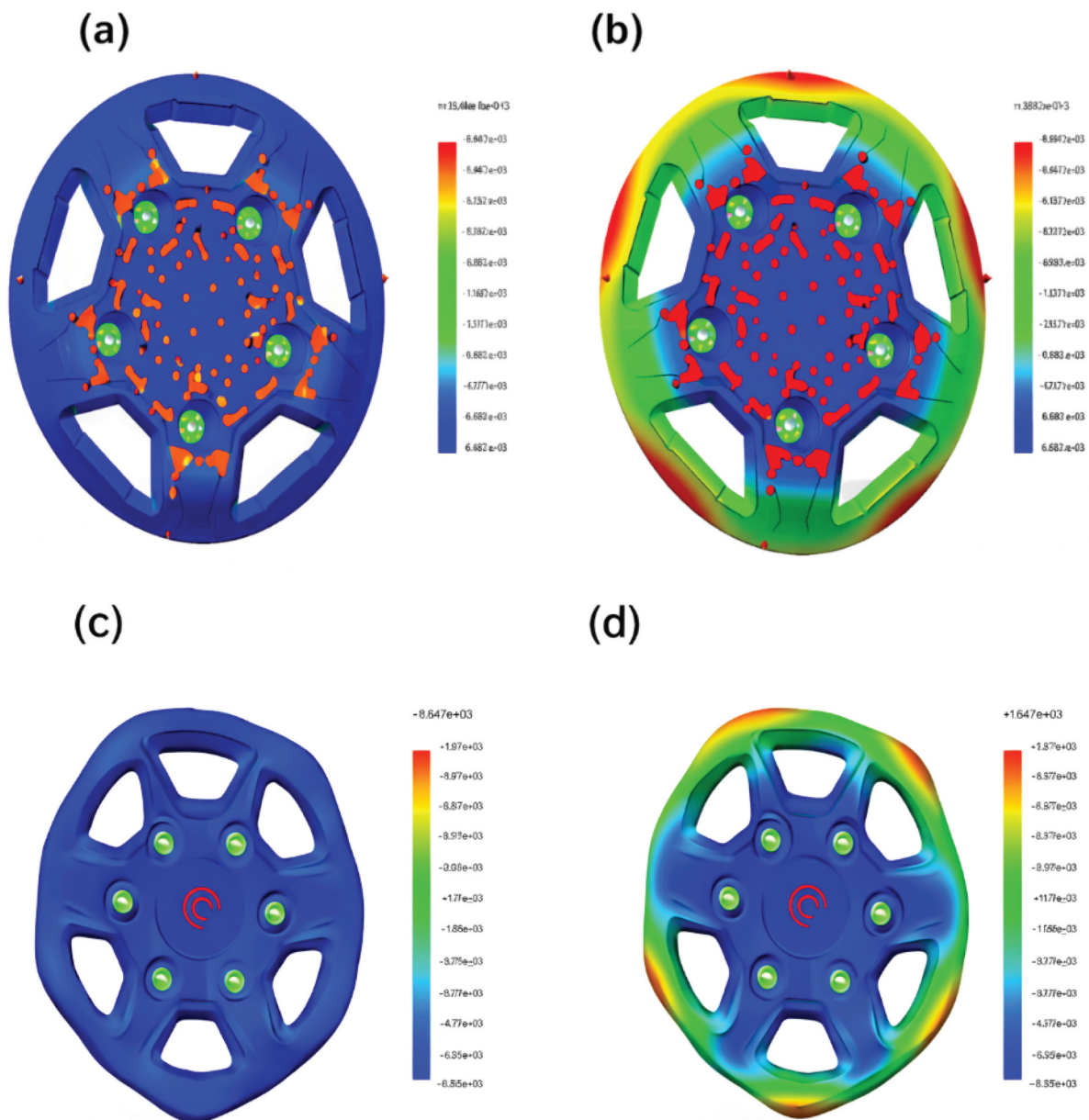


**Figure 9.** Static loading: (a) Von Mises stress distribution; (b) resulting displacement field. Centrifugal loading: (c) Von Mises stress distribution; (d) resulting displacement field.

around the five fixing holes, while the rest of the hubcap remains lightly stressed (Figure 9a). This concentration is expected, since the fixing points are the main load-transfer paths between the hubcap and the wheel, and similar stress patterns have been reported in FE analyses of composite wheel covers and discs. The maximum stress remains well below the measured tensile strength of the jute–epoxy composite (25.97 MPa), indicating a comfortable safety margin for normal service loads. The corresponding displacement field reveals a maximum deflection of only 0.0584 mm, confirming the good global stiffness of the design and suggesting that no visible deformation or rattling is likely to occur in operation (Figure 9b).

For the centrifugal loading case at 2546 rpm, the stress pattern is similar, with peak Von Mises stresses of about 9.5 MPa again concentrated near the fixing regions and peripheral areas where the geometry changes (Figure 9c). The majority of the hubcap surface experiences low to moderate stress levels, indicating that the jute–epoxy laminate can withstand the inertial forces generated during wheel rotation without approaching its strength limit, in line with recent numerical investigations on rotating composite discs and natural-fiber wheels. The predicted displacements, ranging from  $1.0 \times 10^{-3}$  mm to  $3.14 \times 10^{-2}$  mm, remain very small

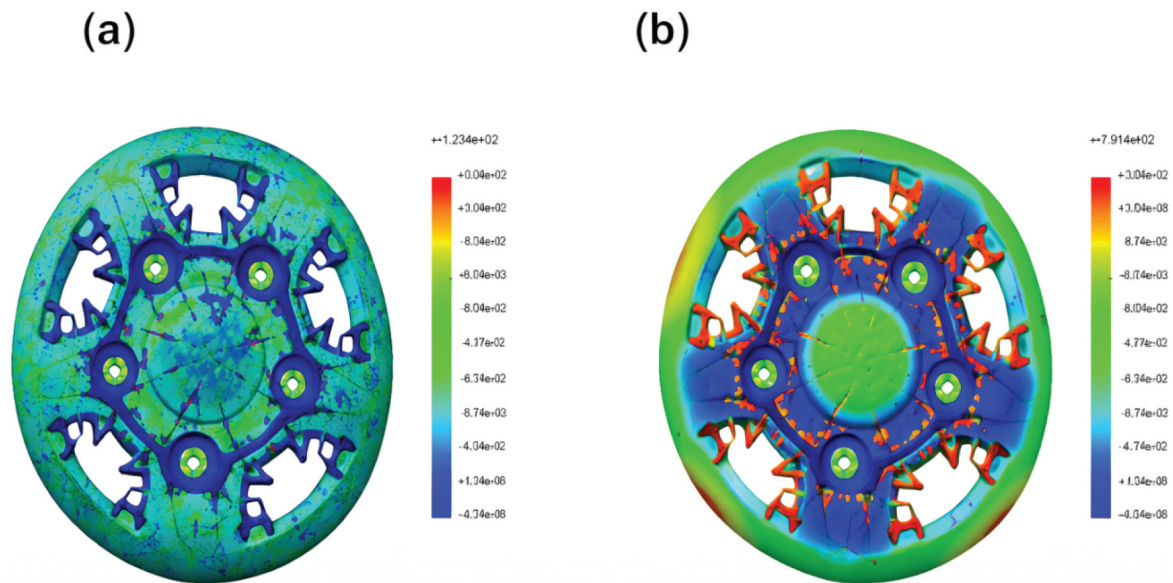


**Figure 10.** Thermal loading (130 °C): (a) Von Mises stress distribution; (b) resulting displacement field.

**Table 1.** Summary of FE results and safety factors for the jute–epoxy hubcap.

Loading case	$\sigma_{max}$ (MPa)	$\sigma_{max}/\sigma_u$ Tensile	Safety factor ( $\approx \sigma_u / \sigma_{max}$ )	$u_{max}$ (mm)
Static mechanical load	8.0	0.31	$\approx 3.2$	0.0584
Centrifugal load (2546 rpm)	9.5	0.37	$\approx 2.7$	0.0314
Thermal load (130°C, uniform)	52.3	2.0	<1	0.138

compared with the overall dimensions of the part (Figure 9d). This confirms that the hubcap maintains its shape and clearance with surrounding components even at elevated rotational speeds.

The thermal loading scenario at 130°C is more severe. In this case, the Von Mises stress varies between 17.3 kPa and 52.3 MPa, with the highest values occurring in the inner segments and geometrically complex regions where thermal expansion is constrained (Figure 10a). The maximum stress slightly exceeds the room-temperature tensile strength measured on the jute–epoxy plates, which suggests that the material could locally reach or surpass its elastic limit at such temperatures, especially if the epoxy matrix approaches its glass transition region. The maximum displacement, about 0.138 mm, remains moderate but higher than in the mechanical cases, reflecting the combined effect of thermal expansion and stiffness reduction (Figure 10b), a behavior also observed in other thermoset-based biocomposites exposed to elevated temperatures.

These results indicate that, while the hubcap behaves satisfactorily under static and centrifugal mechanical loads, its long-term integrity at high temperatures is more critical and depends on the actual service temperature range, exposure duration and potential thermo-oxidative aging of the matrix.

To facilitate comparison between load cases, Table 1 summarizes the maximum Von Mises stress and displacement together with the corresponding safety factors with respect to the measured tensile strength of the jute–epoxy composite.

where  $\sigma_u = 25.97$  MPa is the ultimate tensile strength of the jute–epoxy laminate measured in Governing equations.

### Light-weighting and application potential

The manufactured jute–epoxy hubcap has a measured mass of 239 g for a diameter of 380 mm, which is significantly lower than the typical mass range reported for commercial plastic hubcaps of similar size, generally between 350 and 450 g, depending on design and material (ABS or PP-GF). This corresponds to an estimated weight reduction of approximately 30–40% per wheel. This reduction is mainly attributed to

the relatively low density of jute fibers ( $\approx 1.3\text{--}1.5\text{ g/cm}^3$ ) compared to conventional reinforcements such as glass fibers, as well as to the efficient material distribution achieved through the optimized geometry of the hubcap. Although the hubcap itself is not a major contributor to the total vehicle mass, such reductions, when combined with other lightweight components, can contribute to lower fuel or energy consumption and reduced CO<sub>2</sub> emissions over the vehicle lifetime, as highlighted in life-cycle assessment studies (Klippel 1998, Ullah, Akhter et al. 2025; Volpe and Pantani 2025).

From a functional point of view, the combination of mechanical test data and finite element (FE) simulations shows that the jute–epoxy hubcap can meet the basic structural requirements for a non-structural exterior automotive component. Under typical mechanical loading conditions, the maximum stresses remain well below the tensile strength of the material, while the predicted displacements are very small, indicating good stiffness and dimensional stability. In addition, the hubcap maintains its structural integrity under rotational conditions, confirming its ability to withstand centrifugal effects during service (Mache, Deb, and Gunti 2024; Ullah, Akhter et al. 2025). The main limitation highlighted by the simulations is the sensitivity to high thermal loads. Under elevated temperature conditions (130 °C), the induced stresses may approach or exceed the material strength, which can be associated with the thermo-mechanical limitations of the epoxy matrix, particularly near its glass transition temperature. This suggests that careful selection of the epoxy system, along with possible design adaptations or thermal protection strategies, is required if the component is exposed to prolonged high-temperature environments, such as those encountered near braking systems.

Nevertheless, the results confirm that jute–epoxy biocomposites are viable candidates for lightweight and environmentally friendly wheel-cover applications. They provide a good compromise between mass reduction, mechanical performance, and sustainability. These findings also motivate further work on thermal optimization, durability, and long-term behavior under realistic service conditions, in order to fully exploit the potential of natural fiber composites in automotive applications.

### **Limitations and perspectives**

The present study is limited to quasi-static loading conditions and to a single composite configuration consisting of two woven jute plies embedded in an epoxy matrix with a fixed fiber volume fraction. While this approach provides a first-order assessment of the structural feasibility of the proposed hubcap, it does not fully capture the complexity of real service conditions.

In particular, several important aspects were not addressed and require further investigation. These include impact behavior, such as resistance to stone-chip damage, which is critical for exterior automotive components, as well as fatigue performance under cyclic loading, including repeated bending and centrifugal effects associated with long-term vehicle operation. Additionally, environmental aging phenomena, such as moisture absorption and ultraviolet (UV) exposure, may significantly affect the mechanical properties and durability of natural fiber composites and should be considered in future studies.

From a numerical standpoint, the finite element model relies on an equivalent homogeneous material assumption, which does not account for the inherently orthotropic behavior of woven jute laminates. Moreover, the model does not consider the presence of manufacturing-induced defects, such as voids, fiber misalignment, or local variations in fiber volume fraction, all of which may influence stress distribution, damage initiation, and failure mechanisms in service.

Future work will therefore focus on developing more advanced numerical models incorporating orthotropic material behavior and layered composite formulations, as well as progressive damage and failure criteria. In parallel, further experimental investigations will be conducted to evaluate impact resistance, fatigue life, and long-term durability under combined mechanical, thermal, and environmental loading representative of real driving conditions. These developments are essential to provide a more comprehensive assessment of the performance and reliability of jute–epoxy biocomposites in automotive applications.

### **Conclusion**

This study demonstrated the feasibility of designing, simulating, and manufacturing an automotive hubcap using a woven jute–fabric-reinforced epoxy biocomposite. The composite exhibited a tensile strength of

25.97 MPa, a tensile modulus of 2.47 GPa, and a flexural strength of 69.41 MPa, confirming its suitability for semi-structural applications. Finite element analyses showed maximum Von Mises stresses of 8.0 MPa under static loading and 9.5 MPa under centrifugal loading (2546 rpm), with corresponding displacements of 0.058 mm and 0.031 mm, ensuring safety factors above 2.7. Under thermal loading at 130°C, stresses reached 52.3 MPa with a displacement of 0.138 mm, identifying temperature as the most critical condition.

The compression-molding process enabled the fabrication of a lightweight prototype with a mass of 239 g, achieving an estimated weight reduction of 30–40% compared to conventional hubcaps. These results confirm that jute–epoxy biocomposites are promising candidates for non-structural automotive components. Future work will focus on thermal optimization, impact and fatigue behavior, and long-term durability under realistic service conditions.

## Acknowledgments

The authors acknowledge the financial support through Ongoing Research Funding program (ORF-2026-688), King Saud University, Riyadh, Saudi Arabia.

## Author contributions

CRedit: **Nafissa Moussaoui**: Conceptualization, Formal analysis, Investigation, Methodology, Validation, Writing – original draft; **Salah Amroune**: Formal analysis, Methodology, Supervision, Visualization, Writing – original draft; **Ahmed Belaadi**: Methodology, Validation, Writing – review & editing; **Moussa Zaoui**: Validation, Visualization, Writing – review & editing; **Mohammad Jawaid**: Visualization, Writing – review & editing; **Mahmood M. S. Abdullah**: Visualization, Writing – review & editing; **Hamad A. Al-Lohedan**: Writing – review & editing; **Herbert Mukalazi**: Writing – review & editing; **Amar Al-Khawlan**: Writing – review & editing.

## Disclosure statement

No potential conflict of interest was reported by the author(s).

## ORCID

Salah Amroune  <http://orcid.org/0000-0002-9565-1935>

## Data availability statement

Data will be made available on request.

## Highlights

- Jute–epoxy biocomposite hubcap developed as a lightweight, eco-friendly alternative.
- FE simulations confirm structural integrity under static, centrifugal, and thermal loads.
- Compression molding using a silicone mold ensures controlled fabrication.
- Mechanical tests validate material properties and load-bearing capacity.
- Low deformation observed; thermal loading (130 °C) is the critical condition.

## References

- Abdellaoui, H., H. Bensalah, J. Echaabi, R. Bouhfid, and A. Qaiss. 2015. “Fabrication, Characterization and Modelling of Laminated Composites Based on Woven Jute Fibres Reinforced Epoxy Resin.” *Materials and Design* 68:104–113. <https://doi.org/10.1016/j.matdes.2014.11.059>.
- Akter, M., M. H. Uddin, and I. S. Tania. 2022. “Biocomposites Based on Natural Fibers and Polymers: A Review on Properties and Potential Applications.” *Journal of Reinforced Plastics & Composites* 41 (17–18): 705–742. <https://doi.org/10.1177/07316844211070609>.

- Amroune, S., A. Bezazi, A. Dufresne, F. Scarpa, and A. Imad. 2021. "Investigation of the Date Palm Fiber for Green Composites Reinforcement: Thermo-Physical and Mechanical Properties of the Fiber." *Journal of Natural Fibers* 18 (5): 717–734. <https://doi.org/10.1080/15440478.2019.1645791>.
- Awrejcewicz, J., and V. A. Krysko. 2020. *Elastic and Thermoelastic Problems in Nonlinear Dynamics of Structural Members*. Springer.
- Azwa, Z. N., B. F. Yousif, A. C. Manalo, and W. Karunasena. 2013. "A Review on the Degradability of Polymeric Composites Based on Natural Fibres." *Materials and Design* 47:424–442. <https://doi.org/10.1016/j.matdes.2012.11.025>.
- Belaadi, A., S. Amroune, Y. Seki, O. Y. Keskin, S. Köktaş, M. Bouchak, A. Dufresne, H. Fouad, and M. Jawaid. 2022. "Extraction and Characterization of a New Lignocellulosic Fiber from *Yucca Treculeana* L. Leaf as Potential Reinforcement for Industrial Biocomposites." *Journal of Natural Fibers* 19 (15): 12235–12250. <https://doi.org/10.1080/15440478.2022.2054895>.
- Belaadi, A., M. Boumaaza, S. Amroune, and M. Bouchak. 2020. "Mechanical Characterization and Optimization of Delamination Factor in Drilling Bidirectional Jute Fibre-Reinforced Polymer Biocomposites." *International Journal of Advanced Manufacturing Technology* 111 (7): 2073–2094. <https://doi.org/10.1007/s00170-020-06217-6>.
- Belhocine, A., and O. I. Abdullah. 2020. "Design and Thermomechanical Finite Element Analysis of Frictional Contact Mechanism on Automotive Disc Brake Assembly." *Journal of Failure Analysis & Prevention* 20 (1): 270–301. <https://doi.org/10.1007/s11668-020-00831-y>.
- Benhamadouche, L., N. Moussaoui, A. Benkhelif, M. Jawaid, M. Rokbi, H. Osmani, H. Fouad, and B. Singh. 2025. "Resistance to Crack Propagation of a Composite with Recycled Jute Fabric–Polypropylene." *Composite Structures* 356:118884. <https://doi.org/10.1016/j.compstruct.2025.118884>.
- Benyettou, R., A. Elhadi, S. Amroune, M. Slamani, G. Nyiranzeyimana, B. Louhichi, and A. A. Elfar. 2026. "Optimizing Water Absorption Resistance of Jute Fiber Composites Through Al<sub>2</sub>O<sub>3</sub> Nanoparticle Incorporation: Predictive Modeling Across Multiple Aqueous Environments." *Journal of Natural Fibers* 23 (1): 2653086. <https://doi.org/10.1080/15440478.2026.2653086>.
- Czerwinski, F. 2021. "Current Trends in Automotive Lightweighting Strategies and Materials." *Materials* 14 (21): 6631. <https://doi.org/10.3390/ma14216631>.
- Djalal, M., M. Nafissa, R. Mansour, M. Jawaid, M. Hocine, and B. Lamia. 2024. "Effect of Alkali Treatment on New Lignocellulosic Fibres from the Stem of the *Aster Squamatus* Plant." *Journal of Materials Research and Technology* 32:2882–2890. <https://doi.org/10.1016/j.jmrt.2024.08.104>.
- Dunić, V., N. Busarac, V. Slavković, B. Rosić, R. Niekamp, H. Matthies, R. Slavković, and M. Živković. 2016. "A Thermo-Mechanically Coupled Finite Strain Model Considering Inelastic Heat Generation." *Continuum Mechanics and Thermodynamics* 28 (4): 993–1007. <https://doi.org/10.1007/s00161-015-0442-5>.
- Farronato, D., M. Manfredini, A. Stevanello, V. Campana, L. Azzi, and M. Farronato. 2019. "A Comparative 3D Finite Element Computational Study of Three Connections." *Materials* 12 (19): 3135. <https://doi.org/10.3390/ma12193135>.
- Faruk, O., A. K. Bledzki, H.-P. Fink, and M. Sain. 2012. "Biocomposites Reinforced With Natural Fibers: 2000–2010." *Progress in Polymer Science* 37 (11): 1552–1596. <https://doi.org/10.1016/j.progpolymsci.2012.04.003>.
- Fisher, G. 2023. "Natural Fibers: The New Fashion in Automotive Composites." *International Fiber Journal | Fibers, Filaments & Processing Solutions, International Fiber Journal*.
- Fnides, M., S. Amroune, M. Slamani, B. Louhichi, M. Jawaid, and A. A. Elfar. 2026. "Hybrid Optimization and Predictive Modeling of Mechanical Properties in Treated Natural Palm Fibers for High-Performance Biocomposites." *Cellulose* 33 (6): 3355–3382. <https://doi.org/10.1007/s10570-026-06981-w>.
- Gupta, N. K., N. Somani, G. Nandan, and R. K. Phanden. 2023. "Investigation of the Mechanical Properties of Jute and Glass Fiber Reinforced Epoxy Composite for Sustainable and Cost-Effective Applications." *International Journal on Interactive Design and Manufacturing (IJIDeM)*: 1–14. <https://doi.org/10.1007/s12008-023-01684-z>.
- Haq, E., A. Saifullah, A. Habib, A. Y. M. A. Azim, S. Alimuzzaman, H. N. Dhakal, and F. Sarker. 2024. "Improved Mechanical Properties of Environmentally Friendly Jute Fibre Reinforced Metal Laminate Sandwich Composite Through Enhanced Interface." *Heliyon* 10 (2): e24345. <https://doi.org/10.1016/j.heliyon.2024.e24345>.
- Hasan, M. M., M. A. Islam, and T. Hassan. 2024. "Analysis of Jute-Glass Fiber Reinforced Epoxy Hybrid Composite." *Heliyon* 10 (24): e40924. <https://doi.org/10.1016/j.heliyon.2024.e40924>.
- Hossain, M. R., M. A. Islam, A. Van Vuurea, and I. Verpoest. 2013. "Tensile Behavior of Environment Friendly Jute Epoxy Laminated Composite." *Procedia Engineering* 56:782–788. <https://doi.org/10.1016/j.proeng.2013.03.196>.
- Ibrahim, H. K., M. S. Abolarin, A. S. Abdulrahman, P. O. Omoniyi, R. M. Mahamood, T.-C. Jen, and E. T. Akinlabi. 2025. "Structural Simulation of Ti–Ha–CaCo<sub>3</sub> Biocomposites Using Finite Element Analysis (FEA) for Biomechanical Stability of Hip Implant." *International Journal on Interactive Design and Manufacturing (IJIDeM)* 19 (6): 3999–4012. <https://doi.org/10.1007/s12008-024-01968-y>.
- Islam, M. Z., M. E. Sarker, M. M. Rahman, M. R. Islam, A. T. M. F. Ahmed, M. S. Mahmud, and M. Syduzzaman. 2022. "Green Composites from Natural Fibers and Biopolymers: A Review on Processing, Properties, and Applications." *Journal of Reinforced Plastics & Composites* 41 (13–14): 526–557. <https://doi.org/10.1177/07316844211058708>.
- Joshi, S. V., L. T. Drzal, A. K. Mohanty, and S. Arora. 2004. "Are Natural Fiber Composites Environmentally Superior to Glass Fiber Reinforced Composites?" *Composites, Part A, Applied Science and Manufacturing* 35 (3): 371–376. <https://doi.org/10.1016/j.compositesa.2003.09.016>.

- Kannan, G., R. A. Kurien, R. Thangaraju, V. Shanmugam, S. Rajendran, V. Karupaiah, S. Ramasamy, S. Suttiruengwong, S. M. Rangappa, and S. Siengchin. 2025. "Advances in Cellulosic Natural Fibre-Reinforced Polymer Composites: Properties, Additive Manufacturing and Hybridisation – a Review." *International Journal of Biological Macromolecules* 327:147374. <https://doi.org/10.1016/j.ijbiomac.2025.147374>.
- Kannan, G., R. Thangaraju, S. Suttiruengwong, V. Shanmugam, S. M. Rangappa, K. R. Sumesh, R. A. Kurien, and S. Siengchin. 2025. "Effect of Drilling Process Parameters on Agro-Waste-Based Polymer Composites Reinforced with Banana Fiber and Coconut Shell Filler." *Biomass Conversion and Biorefinery* 15 (9): 13719–13732. <https://doi.org/10.1007/s13399-024-06140-w>.
- Karthika, M. R., A. Deb, and G. S. Venkatesh. 2021. "An Investigation into Mechanical Properties of Jute–Polyester Laminates for Numerical Prediction of Strength and Failure." *Polymer Composites* 42 (11): 5975–5999. <https://doi.org/10.1002/pc.26278>.
- Klippel, B. B. P. 1998. *A Design Methodology for Automotive Component Manufacturing Systems*. Massachusetts Institute of Technology.
- Koppiseti, S. B., R. Nallu, and R. R. Penmetsa. 2022. "Passenger Cars Wheel Performance Test Simulation for Service Life Evaluation: A Review." *Journal of Failure Analysis & Prevention* 22 (4): 1370–1392. <https://doi.org/10.1007/s11668-022-01447-0>.
- Kurien, R. A., and M. Maria Anil. 2023. "Natural Fiber Composites as Sustainable Resources for Emerging Applications - A Review." In *Materials Today: Proceedings*, Kochi, India.
- Kurien, R. A., A. Arshad, A. Joseph, A. Sunil, B. T. Cherian, S. M. Rangappa, S. Suttiruengwong, G. Kannan, and S. Siengchin. 2025. "Agave-Jute Fiber–Reinforced Hybrid Composite for Lightweight Applications: Effect of Hybridization." *Biomass Conversion and Biorefinery* 15 (8): 12241–12254. <https://doi.org/10.1007/s13399-024-05984-6>.
- Kurien, R. A., and A. Biju. 2022. "Chicken Feather Fiber Reinforced Composites for Sustainable Applications." In *Materials Today: Proceedings*, SRM Institute of Science and Technology, Ramapuram Campus, Chennai, Tamil Nadu, India, 58, 862–866.
- Kurien, R. A., M. Bodaghi, N. D. Mathew, M. Paul, S. V. Ravi, and P. Praveen. 2025. "Fabrication, Properties, and Morphologies of Novel Acacia–Jute Hybrid Polymer Composites." *Journal of Composites Science* 9 (7): 316. <https://doi.org/10.3390/jcs9070316>.
- Kurien, R. A., and G. Kannan. 2026. "4 - Processing Methods and Techniques for Eco-Friendly Fibers and Polymers for the Sustainable Environment." In *Eco-Friendly Fiber Reinforced Polymer Composite Materials*, edited by S. M. Rangappa, S. Siengchin, A. L. Leao, and R. M. Kozlowski, 77–107, Cambridge, Royaume-Uni (UK), Woodhead Publishing.
- Kurien, R. A., G. Kannan, G. B. Kurup, G. S. Reji, A. Santhosh, D. Paul, S. M. Rangappa, S. Suttiruengwong, and S. Siengchin. 2024. "Comparative Mechanical and Morphological Characteristics of an Innovative Hybrid Composite of Vetiver and Jute." *Journal of Polymer Research* 31 (12): 356. <https://doi.org/10.1007/s10965-024-04208-9>.
- Kurien, R. A., D. P. Selvaraj, M. Sekar, and C. P. Koshy. 2020. "Green Composite Materials for Green Technology in the Automotive Industry." *IOP Conference Series: Materials Science & Engineering* 872 (1): 012064. <https://doi.org/10.1088/1757-899X/872/1/012064>.
- Kurien, R. A., D. P. Selvaraj, M. Sekar, C. P. Koshy, C. Paul, S. Palanisamy, C. Santulli, and P. Kumar. 2023. "A Comprehensive Review on the Mechanical, Physical, and Thermal Properties of Abaca Fibre for Their Introduction into Structural Polymer Composites." *Cellulose* 30 (14): 8643–8664. <https://doi.org/10.1007/s10570-023-05441-z>.
- Kurien, R. A., and M. Thomas. 2026. "Surface-Modified Natural Fiber Composites." In *Natural Fiber Composites for a Sustainable Environment*, edited by J. T. Philip, J. Jose, and S. C. George, 237–249. Boca Raton, FL: CRC Press.
- Lamia, B., M. Nafissa, B. Abdelouahab Djoubair, M. Jawaid, H. Fouad, and M. Midani. 2023. "New Cellulosic Fibre from Spathes of Male Date for Lightweight Composite Materials: Extraction and Characterization." *Journal of Materials Research and Technology* 24:5361–5371. <https://doi.org/10.1016/j.jmrt.2023.04.159>.
- Mache, A., A. Deb, and R. S. Gunti. 2024. "Predictive Modeling of Jute-Polyester Composite Tubes for Impact Performance: A Comprehensive Finite Element Analysis Approach." *Polymer Composites* 45 (3): 2171–2188. <https://doi.org/10.1002/pc.27911>.
- Madueke, C. I., O. M. Mbah, and R. Umunakwe. 2023. "A Review on the Limitations of Natural Fibres and Natural Fibre Composites with Emphasis on Tensile Strength Using Coir as a Case Study." *Polymer Bulletin* 80 (4): 3489–3506. <https://doi.org/10.1007/s00289-022-04241-y>.
- Mir, A., R. Zitoun, F. Collombet, and B. Bezzazi. 2010. "Study of Mechanical and Thermomechanical Properties of Jute/Epoxy Composite Laminate." *Journal of Reinforced Plastics & Composites* 29 (11): 1669–1680. <https://doi.org/10.1177/0731684409341672>.
- Mostefa Meddah, S. A., M. Rokbi, A. Belaadi, N. Bouaziz, S. Achour, M. S. A. Mahmood, H. A. Al-Lohedan, A. Al-Khawlani, and H. Mukalazi. 2026. "Comparative Analysis of Polyester Composites Reinforced with Local Plant Fibers: Stipa Tenacissima vs. Agave Americana." *Journal of Natural Fibers* 23 (1): 1–30.

- Moussaoui, N., L. Benhamadouche, Y. Seki, S. Amroune, A. Dufresne, M. Jawaid, and H. Fouad. 2023. "The Impact of Physicochemical Treatments on the Characteristics of Ampelodesmos Mauritanicus Plant Fibers." *Cellulose* 30 (12): 7479–7495. <https://doi.org/10.1007/s10570-023-05377-4>.
- Moussaoui, N., M. Rokbi, H. Osmani, M. Jawaid, A. Atiqah, M. Asim, and L. Benhamadouche. 2021. "Extraction and Characterization of Fiber Treatment Inula Viscosa Fibers as Potential Polymer Composite Reinforcement." *Journal of Polymers and the Environment* 29 (11): 3779–3793. <https://doi.org/10.1007/s10924-021-02147-w>.
- Musa, A. A., and A. P. Onwualu. 2024. "Potential of Lignocellulosic Fiber Reinforced Polymer Composites for Automobile Parts Production: Current Knowledge, Research Needs, and Future Direction." *Heliyon* 10 (3): e24683. <https://doi.org/10.1016/j.heliyon.2024.e24683>.
- Naghdi, R. 2021. "Advanced Natural Fibre-Based Fully Biodegradable and Renewable Composites and Nanocomposites: A Comprehensive Review." *International Wood Products Journal* 12 (3): 178–193. <https://doi.org/10.1080/20426445.2021.1945180>.
- Naik, V., and M. Kumar. 2021. "A Review on Natural Fiber Composite Material in Automotive Applications." *Engineered Science* 18 (18): 1–10.
- Pickering, K. L., M. A. Efendy, and T. M. Le. 2016. "A Review of Recent Developments in Natural Fibre Composites and Their Mechanical Performance." *Composites, Part A, Applied Science and Manufacturing* 83:98–112. <https://doi.org/10.1016/j.compositesa.2015.08.038>.
- Puttegowda, M. 2025. "Eco-Friendly Composites: Exploring the Potential of Natural Fiber Reinforcement." *Discover Applied Sciences* 7 (5): 401. <https://doi.org/10.1007/s42452-025-06981-8>.
- Raja, R. N. J., N. J. R. A. Kurien, and S. Jannet. 2025. "3D Printing of Tailored Polymer Composites: Enhancing Sustainability with Banana and Pineapple Fiber Particle Reinforcements." *Engineering Research Express* 7 (2): 025442. <https://doi.org/10.1088/2631-8695/addb2c>.
- Saada, K., S. Amroune, M. Zaoui, A. Houari, K. Madani, and A. Hachaichi. 2023. "Experimental and Numerical Study of the Effect of the Presence of a Geometric Discontinuity of Variable Shape on the Tensile Strength of an Epoxy Polymer." *Acta Mechanica et Automatica* 17 (2): 192–199. <https://doi.org/10.2478/ama-2023-0022>.
- Saba, N., M. Jawaid, O. Y. Alothman, and M. T. Paridah. 2016. "A Review on Dynamic Mechanical Properties of Natural Fibre Reinforced Polymer Composites." *Construction and Building Materials* 106:149–159. <https://doi.org/10.1016/j.conbuildmat.2015.12.075>.
- Sahu, D. P., R. Das, and S. C. Mohanty. 2025. "Multiwalled Carbon Nanotubes Filled Pineapple/Kenaf Hybrid Laminated Composites Structures for Electromagnetic Interface Shielding Applications." *Polymer Composites* 46 (8): 7261–7276. <https://doi.org/10.1002/pc.29428>.
- Sahu, D. P., R. Das, J. K. Prusty, and S. C. Mohanty. 2025a. "Flexural and Dynamic Characterization of Carbon/Basalt Hybrid Laminated Composite Sandwich Plates with PET Foam Core: A Numerical and Experimental Approach." *Structures* 72:108204. <https://doi.org/10.1016/j.istruc.2025.108204>.
- Sahu, D. P., R. Das, J. K. Prusty, and S. C. Mohanty. 2025b. "Tensile, Flexural, and Vibration Analysis of MWCNT-Basalt Sandwich Composites for Car Bonnet Utility." *Polymer Composites* 46 (12): 10842–10863. <https://doi.org/10.1002/pc.29657>.
- Sahu, D. P., S. Kumar, and M. K. Gupta. 2025. "Flexural and Free Vibration Analysis of Glass and Natural Fiber-Based Hybrid Laminated Composites: Experimental and Numerical Insights." *Fibers and Polymers* 26 (4): 1765–1782. <https://doi.org/10.1007/s12221-025-00902-7>.
- Sahu, D. P., and S. C. Mohanty. 2025. "Static and Dynamic Analysis of Polyethylene Terephthalate Foam Core and Different Natural Fiber-Reinforced Laminated Composite-Based Sandwich Plates Through Experimental and Numerical Simulation." *Mechanics of Advanced Materials and Structures* 32 (13): 3066–3085. <https://doi.org/10.1080/15376494.2024.2388275>.
- Sánchez-Majano, A. R., R. Masia, A. Pagani, and E. Carrera. 2022. "Microscale Thermo-Elastic Analysis of Composite Materials by High-Order Geometrically Accurate Finite Elements." *Composite Structures* 300:116105. <https://doi.org/10.1016/j.compstruct.2022.116105>.
- Saravanakumar, Y. N., and N. K. Chandran. 2026. "Chapter 1 - Recent Developments in Natural Fibre-Reinforced Polymer Biocomposites for Future Sustainability and Key Challenges: A Review." In *Damage Analysis of Natural Fiber-Reinforced Polymer Biocomposites*, edited by M. T. HAMEED, Sultan, A. E. K. Qaiss, R. Bouhfid, M. H. MAT. Yazik, and F. SYAZWANI. Shahar, 3–20. Elsevier: Woodhead Publishing.
- Shinde, D., M. Bulsara, and J. Patil. 2022. "Wear Analysis of Eco-Friendly Non-Asbestos Friction-Lining Material Applied in an Automotive Drum Brake: Experimental and Finite-Element Analysis." *Proceedings of the Institution of Mechanical Engineers, Part J: Journal of Engineering Tribology* 236 (3): 552–562. <https://doi.org/10.1177/13506501211016730>.
- Siguerdjijene, H., A. Houari, K. Madani, S. Amroune, M. Mokhtari, B. Mohamad, C. Ahmed, A. Merah, and R. Campilho. 2024. "Predicting Damage in Notched Functionally Graded Materials Plates Through Extended Finite Element Method Based on Computational Simulations." *Fracture and Structural Integrity* 18 (70): 1–23. <https://doi.org/10.3221/IGF-ESIS.70.01>.
- Sivaraja, M., K. Kandasamy, N. Velmani, and M. S. Pillai. 2010. "Study on Durability of Natural Fibre Concrete Composites Using Mechanical Strength and Microstructural Properties." *Bulletin of Materials Science* 33 (6): 719–729. <https://doi.org/10.1007/s12034-011-0149-6>.

- Skosana, S. J., C. Khoathane, and T. Malwela. 2025. "Driving Towards Sustainability: A Review of Natural Fiber Reinforced Polymer Composites for Eco-Friendly Automotive Light-weighting." *Journal of Thermoplastic Composite Materials* 38 (2): 754–780. <https://doi.org/10.1177/08927057241254324>.
- Slamani, M., A. Elhadi, S. Amroune, M. Arslane, O. Y. Alothman, O. Awayssa, J.-F. Chatelain, and M. Jawaid. 2025. "Analysis of Entry and Exit Hole Delaminations During Drilling of Jute/Palm Fiber Reinforced Hybrid Composites Using HSS Drill Bits." *Journal of Natural Fibers* 22 (1): 2461493. <https://doi.org/10.1080/15440478.2025.2461493>.
- Ullah, S., Z. Akhter, A. Palevicius, and G. Janusas. 2025. "Review: Natural Fiber-Based Biocomposites for Potential Advanced Automotive Applications." *Journal of Engineered Fibers and Fabrics* 20:15589250241311468. <https://doi.org/10.1177/15589250241311468>.
- Volpe, V., and R. Pantani. 2025. "Natural Fiber-Reinforced Light Composites for the Automotive Industry." *Polymer Composites* 46 (9): 8660–8673. <https://doi.org/10.1002/pc.29518>.
- Yan, L., and H. Xu. 2025. "Lightweight Composite Materials in Automotive Engineering: State-of-the-Art and Future Trends." *Alexandria Engineering Journal* 118:1–10. <https://doi.org/10.1016/j.aej.2024.12.002>.